

Reversal of domain wall chirality with ferromagnet thickness in W/(Co)FeB/MgO systems

著者	Takaaki Dohi, Samik DuttaGupta, Shunsuke Fukami, Hideo Ohno
journal or publication title	Applied Physics Letters
volume	114
number	4
page range	042405
year	2019-01-31
URL	http://hdl.handle.net/10097/00128368

doi: 10.1063/1.5084095

Reversal of domain wall chirality with ferromagnet thickness in W/(Co)FeB/MgO systems

Cite as: Appl. Phys. Lett. **114**, 042405 (2019); <https://doi.org/10.1063/1.5084095>

Submitted: 04 December 2018 . Accepted: 14 January 2019 . Published Online: 31 January 2019

Takaaki Dohi , Samik DuttaGupta , Shunsuke Fukami, and Hideo Ohno 



View Online



Export Citation



CrossMark

ARTICLES YOU MAY BE INTERESTED IN

[Spin-orbit torque-induced switching of in-plane magnetized elliptic nanodot arrays with various easy-axis directions measured by differential planar Hall resistance](#)

Applied Physics Letters **114**, 012410 (2019); <https://doi.org/10.1063/1.5075542>

[Spin-orbit torques in high-resistivity-W/CoFeB/MgO](#)

Applied Physics Letters **112**, 192408 (2018); <https://doi.org/10.1063/1.5027855>

[Field-free spin-orbit torque switching of a perpendicular ferromagnet with Dzyaloshinskii-Moriya interaction](#)

Applied Physics Letters **114**, 022401 (2019); <https://doi.org/10.1063/1.5052194>

Lock-in Amplifiers
up to 600 MHz



Watch



Reversal of domain wall chirality with ferromagnet thickness in W/(Co)FeB/MgO systems

Cite as: Appl. Phys. Lett. **114**, 042405 (2019); doi: [10.1063/1.5084095](https://doi.org/10.1063/1.5084095)
Submitted: 04 December 2018 · Accepted: 14 January 2019 · Published Online:
31 January 2019



View Online



Export Citation



CrossMark

Takaaki Dohi,¹  Samik DuttaGupta,^{1,2,3,4}  Shunsuke Fukami,^{1,2,3,4,5,6,a)} and Hideo Ohno^{1,2,3,4,5,6} 

AFFILIATIONS

¹ Laboratory for Nanoelectronics and Spintronics, Research Institute of Electrical Communication, Tohoku University, Sendai 980-8577, Japan

² Center for Spintronics Integrated Systems, Tohoku University, Sendai 980-8577, Japan

³ Center for Spintronics Research Network, Tohoku University, Sendai 980-8577, Japan

⁴ Center for Science and Innovation in Spintronics (Core Research Cluster), Tohoku University, Sendai 980-8577, Japan

⁵ Center for Innovative Integrated Electronic Systems, Tohoku University, Sendai 980-0845, Japan

⁶ WPI-Advanced Institute for Materials Research, Tohoku University, Sendai 980-8577, Japan

a) Author to whom correspondence should be addressed: s-fukami@iec.tohoku.ac.jp

ABSTRACT

We investigate the effect of the Dzyaloshinskii-Moriya interaction (DMI) on domain wall (DW) configurations in W/(Co)FeB/MgO structures with varying ferromagnet (FM) thicknesses. The DW chirality and effective DMI field are evaluated from field-induced DW motion. The results indicate a reversal of DW chirality with the FM thickness irrespective of the FM material (CoFeB or FeB) and the crystallographic phase of W (α or β phase). The observed change in the magnitude of the DMI field is supported by an additional measurement of spin-orbit torque assisted magnetization switching under in-plane magnetic fields. The present findings offer previously unknown insights into the origin of interfacial DMI and indicate the co-existence of multiple factors governing DW chirality in systems with broken inversion symmetry.

Published under license by AIP Publishing. <https://doi.org/10.1063/1.5084095>

The manifestation of the spin-orbit interaction in systems with broken inversion symmetry is prospective for future spintronic devices.¹⁻³ In-plane current applied to heavy-metal (HM)/ferromagnet (FM) heterostructures with spin-orbit coupling generates spin-orbit torques (SOT) which allow efficient magnetization switching.⁴⁻⁶ In addition, the spin-orbit interaction at interfaces in broken inversion-symmetry systems gives rise to another effect commonly referred to as the interfacial Dzyaloshinskii-Moriya interaction (DMI).^{7,8} Interfacial DMI tends to stabilize non-collinear spin configurations (for instance, Néel-type domain walls (DWs)^{9,10} and skyrmions¹¹⁻¹³) which can be efficiently driven by the SOT.¹⁴⁻¹⁶ Accordingly, the understanding and tailoring of interfacial DMI in HM/FM structures is of considerable importance towards utilization of these physical phenomena in such magnetic heterostructures. At present, a variety of different models¹⁷⁻²⁵ including the orbital hybridization of electronic states between HM and FM¹⁷⁻¹⁹ and the Rashba-Edelstein effect,²⁰⁻²² have been proposed to describe the microscopic origin of the interfacial DMI. However, lack of a

unified and clear understanding persists, requiring deeper insights into the mechanism of DMI in HM/FM structures.

HM/FM heterostructures utilizing W (as the HM layer) are a promising material system for spin-orbitronics owing to a significantly large SOT²⁶⁻²⁸ and an appreciable DMI strength²⁹ which varies with the composition of the ferromagnet.³⁰ Meanwhile, CoFeB/MgO is beneficial for smooth motion of DWs³¹ and skyrmions³⁰ and a high tunnel magnetoresistance ratio.³² Despite these promising features, interfacial DMI in W/CoFeB/MgO has posed a puzzling question concerning DW chirality. Separate experimental results showed a formation of both left-handed/counter-clockwise³³ and right-handed/clockwise^{29,30,34} chiral DWs. The structural phase (α/β phase) of W was found to affect the magnitude of interfacial DMI and interfacial magnetic anisotropy, although the sign of DMI, or chirality direction, is unchanged.³³ Thus, the factors governing the magnitude and the sign of DMI and DW chirality in W/CoFeB heterostructures remain unclear. Here, we systematically investigate the FM thickness dependence of DMI and DW chirality in

W/CoFeB (or FeB) heterostructures by magnetic field-induced DW motion^{35,36} and SOT-assisted magnetization switching.³⁷ We show a cross-over from right-handed to left-handed DW chirality with varying FM thicknesses. Possible mechanisms to describe this behavior are discussed.

Figure 1(a) shows a three series of stack structures used in this study, i.e., sub./ α -W(4)/Co_{0.19}Fe_{0.56}B_{0.25}(t)/MgO(1.6) (series A, hereafter), sub./ β -W(4)/Co_{0.19}Fe_{0.56}B_{0.25}(t)/MgO(1.6) (series B, hereafter), and sub./ α -W(4)/Fe_{0.75}B_{0.25}(t)/MgO(1.6)/Ta(2) (series C, hereafter), with various FM thicknesses t (numbers in parentheses denote the nominal thickness in nm). The stacks are deposited by dc and rf magnetron sputtering on thermally oxidized Si substrates. The crystallographic phase of W (α or β phase) is controlled by the sputtering condition.²⁷ Magnetization measurements and thermally activated DW motion measurements are carried out for blanket films, while SOT-assisted magnetization switching is measured from 50- μ m-long and 10- μ m-wide Hall-bar devices fabricated by photolithography and Ar-ion milling. Stacks are annealed at 300 °C for 1h. Magnetization measurements indicate the perpendicular easy axis in all the structures. The spontaneous magnetization M_S is determined to be 1.31T, 1.35T, and 1.75 T for series A, B, and C, respectively. A linear extrapolation of the relationship between the areal magnetic moment and the FM thickness reveals an existence of a magnetic dead layer with the thickness (t_d) of 0.24–0.38 nm, in consistent with a previous study.³⁸ Figure 1(b) shows the variation of areal effective anisotropy energy density $K_{\text{eff}}t_{\text{eff}}$ as a function of the effective FM thickness $t_{\text{eff}} (= t - t_d)$. The FeB system shows a larger $K_{\text{eff}}t_{\text{eff}}$ compared to the CoFeB system, which is also consistent with a previous work.³⁹

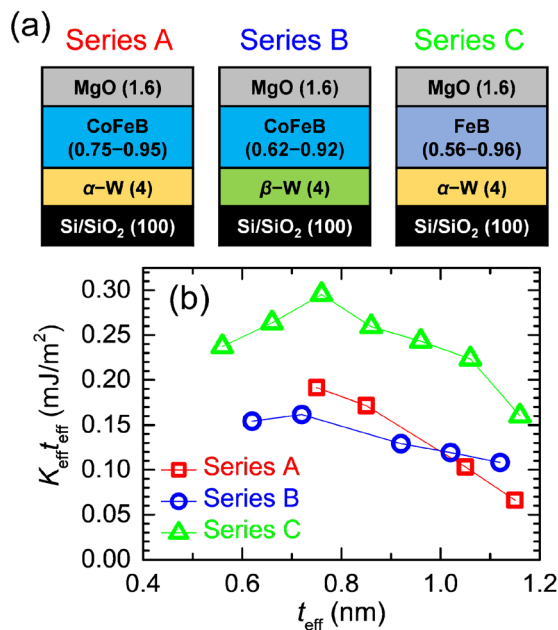


FIG. 1. (a) Schematic diagram of the stack structures and (b) effective areal magnetic anisotropy energy density $K_{\text{eff}}t_{\text{eff}}$ versus effective FM thickness t_{eff} for series A, B, and C.

Next, we evaluate the effective DMI field H_{DMI} from DW motion utilizing magneto-optical Kerr effect microscopy. Starting from a nucleated bubble domain, we measure DW propagation and consequently DW velocity (v_{DW}) under an out-of-plane pulsed magnetic field (H_z). v_{DW} is found to follow sub-threshold behavior for applied $\mu_0 H_z \leq 1.6$ mT (μ_0 is the permeability in free space),^{31,40,41} while presumably moving into depinning or flow regimes for $\mu_0 H_z \geq 1.6$ mT (see [supplementary material](#) for details). The DW chirality and H_{DMI} can be identified from a measurement of DW motion under simultaneous application of dc in-plane magnetic fields (H_x) and H_z pulses. The chiral interactions act as an effective in-plane magnetic field and may be quantified from a minimum in v_{DW} vs H_x either in creep³⁵ or flow regimes.^{42,43} Since several recent studies pointed out that in some cases this approach does not allow an unambiguous determination of H_{DMI} in the creep regime^{42–46} due to an anti-symmetric contribution to v_{DW} , which is negligible in depinning and flow regimes,^{42,43} we apply a large enough H_z to keep DW propagation in depinning or flow regimes. Figures 2(a) and 2(b) show the area traversed by the DW under H_x and H_z for samples with $t_{\text{eff}} = 0.86$ and 0.56 nm in series C [W/FeB(0.86) and W/FeB(0.56), hereafter], respectively. The application of H_x results in an asymmetric domain expansion due to the DMI as expected. Figures 2(c) and 2(d) show v_{DW} ($\uparrow\downarrow$ and $\downarrow\uparrow$ DWs) vs H_x at $\mu_0 H_z = 11.8$ mT for W/FeB(0.86) and at $\mu_0 H_z = 6.5$ mT for W/FeB(0.56), respectively. Interestingly, the results indicate an opposite chirality between them: a left-handed/counter-clockwise chirality ($\uparrow\leftarrow\downarrow$) for W/FeB(0.86) [Fig. 2(c)] and right-handed/clockwise chirality ($\uparrow\rightarrow\downarrow$) for W/FeB(0.56) [Fig. 2(d)].

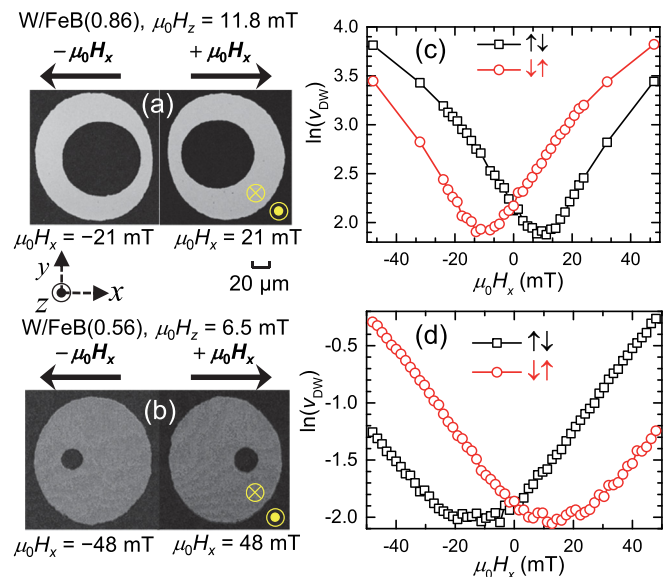


FIG. 2. (a) Magnetic bubble expansion by the applied $\mu_0 H_z$ of 11.8 mT for $t_{\text{eff}} = 0.86$ nm and (b) $\mu_0 H_z$ of 6.5 mT for $t_{\text{eff}} = 0.56$ nm in series C, where the arrow in the image represents the applied direction of H_x and \odot and \otimes denote the up and down magnetic domains, respectively. (c) $\mu_0 H_x$ dependence of v_{DW} for $t_{\text{eff}} = 0.86$ nm in series C under the $\mu_0 H_z$ value of 11.8 mT and (d) that for $t_{\text{eff}} = 0.56$ nm in series C under 6.5 mT.

Figure 3 summarizes the t_{eff} dependence of H_{DMI} . Intriguingly, H_{DMI} continuously decreases with increasing t_{eff} and changes the sign at $t_{\text{eff}} \approx 0.75\text{--}0.85$ nm. The reversal of DW chirality is insensitive to either the FM material (CoFeB or FeB) or the crystallographic phase of W (α or β phase) and does not correlate with $K_{\text{eff}}t_{\text{eff}}$. Thus, the results suggest a possibility of unexplored mechanisms that are responsible for interfacial DMI in HM/FM heterostructures.

To confirm the interfacial nature of H_{DMI} vs t_{eff} , we also investigate H_{DMI} from the in-plane magnetic field dependence of SOT-assisted magnetization switching.³⁷ An in-plane current flowing in the HM/FM heterostructure with a perpendicular easy axis generates an out-of-plane effective field H_{eff}^z that acts on the magnetization of DW and is given by

$$H_{\text{eff}}^z = \chi J$$

$$\chi = \chi'(\cos\theta_{\uparrow\downarrow} + \cos\theta_{\downarrow\uparrow})/2, \quad (1)$$

where J denotes the current density in the HM layer, χ corresponds to the efficiency of Slonczewski-like SOT, $\chi' = (\hbar/2e)(\xi_{\text{SL}}/M_S t_{\text{eff}})$, \hbar is the Dirac constant, e is the electron charge, ξ_{SL} represents the effective spin-Hall-induced torque efficiency, and $\theta_{\uparrow\downarrow}$ and $\theta_{\downarrow\uparrow}$ corresponds to the DW configuration for up to down ($\uparrow\downarrow$) and down to up ($\downarrow\uparrow$) DWs, respectively. According to Eq. (1), H_{eff}^z is cancelled out between opposite DWs ($\uparrow\downarrow$ and $\downarrow\uparrow$) at zero H_x . An increase in H_x gradually aligns magnetization in DW collinear to H_x with an increase in χ and at $H_x \geq H_{\text{DMI}}$, DWs fully align with H_x , leading to maximum χ . Thus, the measurement of SOT-induced magnetization switching under H_x allows us to quantify H_{DMI} . Note that this method is not capable of determining the sign of DMI. For these measurements, we use μm -sized Hall bar devices as shown schematically in Fig. 4(a). Figure 4(b) shows the results of SOT-assisted magnetization switching for W/FeB(0.56) (series C) under $\mu_0 H_x = 50$ mT and dc current $I = \pm 15$ mA. H_{eff}^z is determined as H_z , causing 50% switching (probed by the peak of the derivative of anomalous Hall resistance R_{AHE}). The current dependence of H_{eff}^z is confirmed to obey a linear relation, indicating that the observed effective fields are induced by the current (see supplementary material).

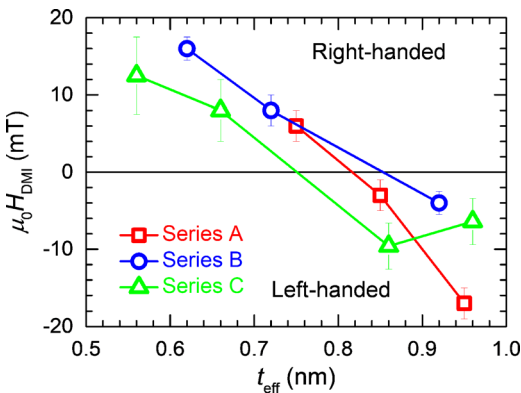


FIG. 3. Effective FM (CoFeB or FeB) thickness dependence of the effective DMI field H_{DMI} for all the series. Error bars of $\mu_0 H_{\text{DMI}}$ are obtained from three measurements on the arbitrary selected different bubbles.

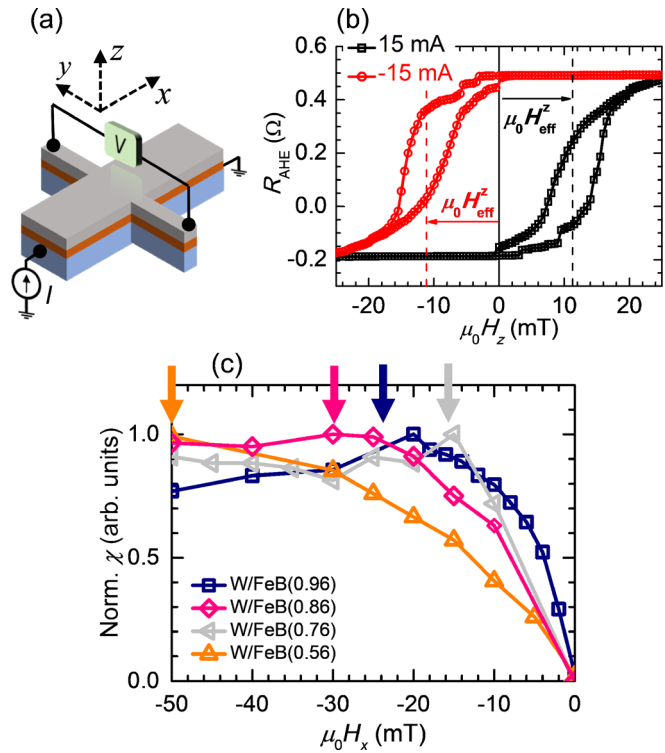


FIG. 4. (a) Schematic diagram of the Hall-bar device. (b) Hall resistance (R_{AHE}) vs out-of-plane magnetic field (H_z) under $\mu_0 H_x = 50$ mT and dc $I = \pm 15$ mA for W/FeB(0.56) (series C). (c) Effective FM thickness (t_{eff}) dependence of normalized SOT efficiency (χ) for series C.

Similar experiments are carried out for all the studied structures. Figure 4(c) summarizes the H_x dependence of normalized χ [$= \chi(H_x)/\chi(0) - 1$]. It is found that the magnitude of H_{DMI} (corresponding to the saturation of H_x indicated by arrows) decreases with the increasing FM thickness. The observed results agree with what we found in DW motion measurements (Fig. 3). These results elucidate the existence of an unknown mechanism for the manifestation of DMI in HM/FM structures and call for further experimental and theoretical investigations.

We now discuss possible scenarios that describe the observed reversal of DW chirality. Previous experimental results supplemented by microscopic models for DMI in $3d\text{--}5d$ bilayer heterostructures have suggested that DMI in HM/FM/oxide trilayer systems originates from the HM/FM interface and is virtually independent of the FM/oxide interface.¹⁹ Experimental results using Pt/FM bilayer structures follow this trend, where an enhancement of the FM thickness merely decreases DMI.⁴⁷ Recently, several experimental studies have revealed an important role of orbital asphericity, where the sign of DMI is determined by $5d$ band filling of the HM layer through the spin-flip process.^{17–19,48,49} Accordingly, in the present case, since the band filling of W is close to the half-filled state, DMI is expected to be sensitive to additional factors such as Rashba interactions,^{20–22} the impact of the usually neglected FM/oxide interface,⁵⁰ and atomic diffusion during annealing.⁵¹ Based on these assumptions,

we propose three possible scenarios that can account for the observed results. One possible contribution arises from charge transfer from O atoms to the thin FM layer, which is capable of modification of $3d$ – $5d$ hybridized bands at the HM/FM interface.⁵⁰ A variation of t_{eff} , then, results in a modified impact of O, which could modify DMI and DW chirality. A similar modification of DMI is also expected from effects of strain in the multilayered heterostructure; however, we may exclude this possibility owing to the independence of our results on the phase of the underlying W layer. The second contribution arises from the possible effects of Rashba effect-induced DMI arising from the FM/oxide interface.²¹ First-principles calculations suggest the presence of Rashba-induced DMI with left-handed/counter-clockwise chirality at the Co/MgO interface.²¹ This is consistent with the DW chirality for thicker t_{eff} in our stacks. On the other hand, the $3d$ – $5d$ hybridization (orbital anisotropy) mechanism suggests that right-handed/clockwise chirality is slightly preferable at the W/FM interface.⁴⁸ Thus, following the second scenario, our experimental results indicate that for thicker samples ($t_{\text{eff}} \geq 0.8$ nm), the contribution of Rashba-induced DMI at the FM/oxide interface becomes dominant and overcomes the contribution from $3d$ – $5d$ hybridization at the HM/FM interface, leading to a reversal of left-handed/counter-clockwise DW chirality. It is worth noting here that the sign reversal of DMI with varying FM thicknesses was not observed in the W/CoFeB/SiO₂ system.⁵² This implies that the MgO layer could play a key role in the sign reversal of DW chirality in W/(Co)FeB heterostructures. The third scenario is related to the diffusion of B into the W and/or MgO layer via annealing. Previous studies report both directions of chirality in similar systems: right-handed chirality in Ta/CoFeB/MgO⁵¹ or TaOx⁵³ and left-handed chirality in Ta/CoFe/MgO.⁵⁴ It has also been pointed out that interdiffusion of B plays a key role in determining the sign of DMI in the Ta/CoFeB/MgO structure.⁵¹ In our case, since the total amount of B accommodated in (Co)FeB depends on the FM thickness, the interdiffusion of B could be a possible factor for the observed sign change. Overall, our results suggest the competition of a number of mechanisms, resulting in the sign reversal of DMI by varying FM thicknesses.

In summary, we have investigated the t_{eff} dependence of the DW chirality and H_{DMI} in W/(Co)FeB/MgO systems by both thermally activated DW motion and SOT-assisted magnetic field switching. The results indicate right-handed/clockwise chiral DWs for the thinner FM layer which changes to a left-handed/counter-clockwise configuration with an increase in the FM thickness. The results suggest a competition of multiple factors such as the conventional $3d$ – $5d$ band hybridization at the W/(Co)FeB interface and Rashba-induced DMI at the FM/MgO interface. The present findings shed light on the underlying physics of the interfacial DMI and direct the proper engineering of material systems for spin-orbitronic applications.

See [supplementary material](#) for (S1) the out-of-plane magnetic field dependence of magnetic bubble expansion and (S2) spin-orbit torque assisted magnetization switching by the magnetic field.

The authors thank Y. Takeuchi, J. Llandro, T. Hirata, H. Iwanuma, and K. Goto for discussion and technical support. This work was supported in part by the ImPACT Program of CSTI, JST-OPERA, JSPS KAKENHI 17H06511/18KK0143, the Core-to-Core Program of JSPS, and Cooperative Research Projects of RIEC. T.D. acknowledges the financial support from the GP-Spin and DIARE of Tohoku University.

REFERENCES

- A. Soumyanarayanan, N. Reyren, A. Fert, and C. Panagopoulos, *Nature* **539**, 509 (2016).
- S. Fukami and H. Ohno, *Jpn. J. Appl. Phys.* **56**, 0802A1 (2017).
- A. Manchon, I. M. Miron, T. Jungwirth, J. Sinova, J. Zelezny, A. Thiaville, K. Garello, and P. Gambardella, preprint [arXiv:1801.09636](#) (2018).
- I. M. Miron, K. Garello, G. Gaudin, P. J. Zermatten, M. V. Costache, S. Auffret, S. Bandiera, B. Rodmacq, A. Schuhl, and P. Gambardella, *Nature* **476**, 189 (2011).
- L. Liu, C.-F. Pai, Y. Li, H. W. Tseng, D. C. Ralph, and R. A. Buhrman, *Science* **336**, 555 (2012).
- S. Fukami, T. Anekawa, C. Zhang, and H. Ohno, *Nat. Nanotechnol.* **11**, 621 (2016).
- I. Dzyaloshinsky, *J. Phys. Chem. Solids* **4**, 241 (1958).
- T. Moriya, *Phys. Rev.* **120**, 91 (1960).
- M. Heide, G. Bihlmayer, and S. Blügel, *Phys. Rev. B* **78**, 140403(R) (2008).
- A. Thiaville, S. Rohart, E. Jué, V. Cros, and A. Fert, *Europhys. Lett.* **100**, 57002 (2012).
- S. Heinze, K. von Bergmann, M. Menzel, J. Brede, A. Kubetzka, R. Wiesendanger, G. Bihlmayer, and S. Blügel, *Nat. Phys.* **7**, 713 (2011).
- A. Fert, V. Cros, and J. Sampaio, *Nat. Nanotechnol.* **8**, 152 (2013).
- C. M. Luchaire, C. Moutas, N. Reyren, J. Sampaio, C. A. F. Vaz, N. V. Horne, K. Bouzehouane, K. Garcia, C. Deranlot, P. Warnicke, P. Wohlhüter, J.-M. George, M. Weigand, J. Raabe, V. Cros, and A. Fert, *Nat. Nanotechnol.* **11**, 444 (2016).
- S. Emori, U. Bauer, A.-M. Ahn, E. Martinez, and G. S. D. Beach, *Nat. Mater.* **12**, 611 (2013).
- K.-S. Ryu, L. Thomas, S.-H. Yang, and S. Parkin, *Nat. Nanotechnol.* **8**, 527 (2013).
- S. Woo, K. Litzius, B. Krüger, M.-Y. Im, L. Caretta, K. Richter, M. Mann, A. Krone, R. M. Reeve, M. Weigand, P. Agrawal, I. Lemesch, M.-A. Mawass, P. Fischer, M. Kläui, and G. S. D. Beach, *Nat. Mater.* **15**, 501 (2016).
- A. Fert and P. M. Levy, *Phys. Rev. Lett.* **44**, 1538 (1980).
- V. Kashid, T. Schena, B. Zimmermann, Y. Mokrousov, S. Blügel, V. Shah, and H. G. Salunke, *Phys. Rev. B* **90**, 054412 (2014).
- S. Kim, K. Ueda, G. Go, P.-H. Jang, K.-J. Lee, A. Belabbes, A. Manchon, M. Suzuki, Y. Kotani, T. Nakamura, K. Nakamura, T. Koyama, D. Chiba, K. T. Yamada, D.-H. Kim, T. Moriyama, K.-J. Kim, and T. Ono, *Nat. Commun.* **9**, 1648 (2018).
- K.-W. Kim, H.-W. Lee, K.-J. Lee, and M. D. Stiles, *Phys. Rev. Lett.* **111**, 216601 (2013).
- H. Yang, O. Boulle, V. Cros, A. Fert, and M. Chshiev, *Sci. Rep.* **8**, 12356 (2018).
- H. Yang, G. Chen, A. A. C. Cotta, A. T. N'Diaye, S. A. Nikolaev, E. A. Soares, W. A. A. Macedo, K. Liu, A. K. Schmid, A. Fert, and M. Chshiev, *Nat. Mater.* **17**, 605 (2018).
- T. Kikuchi, T. Koretsune, R. Arita, and G. Tatara, *Phys. Rev. Lett.* **116**, 247201 (2016).
- G. V. Karnad, F. Freimuth, E. Martinez, R. Lo Conte, G. Gubbiotti, T. Schulz, S. Senz, B. Ocker, Y. Mokrousov, and M. Kläui, *Phys. Rev. Lett.* **121**, 147203 (2018).
- N. Kato, M. Kawaguchi, Y.-C. Lau, and M. Hayashi, preprint [arXiv:1806.07746](#) (2018).
- C.-F. Pai, L. Liu, Y. Li, H. W. Tseng, D. C. Ralph, and R. A. Buhrman, *Appl. Phys. Lett.* **101**, 122404 (2012).
- C. Zhang, S. Fukami, K. Watanabe, A. Ohkawara, S. DuttaGupta, H. Sato, F. Matsukura, and H. Ohno, *Appl. Phys. Lett.* **109**, 192405 (2016).

- ²⁸Y. Takeuchi, C. Zhang, A. Okada, H. Sato, S. Fukami, and H. Ohno, *Appl. Phys. Lett.* **112**, 192408 (2018).
- ²⁹J. Torrejon, J. Kim, J. Sinha, S. Mitani, M. Hayashi, M. Yamanouchi, and H. Ohno, *Nat. Commun.* **5**, 4655 (2014).
- ³⁰S. Jaiswal, K. Litzius, I. Lemesch, F. Büttner, S. Finizio, J. Raabe, M. Weigand, K. Lee, J. Langer, B. Ocker, G. Jakob, G. S. D. Beach, and M. Kläui, *Appl. Phys. Lett.* **111**, 022409 (2017).
- ³¹C. Burrowes, N. Vernier, J.-P. Adam, L. H. Diez, K. Garcia, I. Barisic, G. Agnus, S. Eimer, J.-V. Kim, T. Devolder, A. Lamperti, R. Mantovan, B. Ockert, E. E. Fullerton, and D. Ravelosona, *Appl. Phys. Lett.* **103**, 182401 (2013).
- ³²S. Ikeda, K. Miura, H. Yamamoto, K. Mizunuma, H. D. Gan, M. Endo, S. Kanai, J. Hayakawa, F. Matsukura, and H. Ohno, *Nat. Mater.* **9**, 721 (2010).
- ³³G. W. Kim, A. S. Samardak, Y. J. Kim, I. H. Cha, A. V. Ognev, A. V. Sadovnikov, S. A. Nikitov, and Y. K. Kim, *Phys. Rev. Appl.* **9**, 064005 (2018).
- ³⁴I. Gross, L. J. Martinez, J.-P. Tetienne, T. Hingant, J.-F. Roch, K. Garcia, R. Soucaille, J. P. Adam, J.-V. Kim, S. Rohart, A. Thiaville, J. Torrejon, M. Hayashi, and V. Jacques, *Phys. Rev. B* **94**, 064413 (2016).
- ³⁵S.-G. Je, D.-H. Kim, S.-C. Yoo, B.-C. Min, K.-J. Lee, and S.-B. Choe, *Phys. Rev. B* **88**, 214401 (2013).
- ³⁶R. Lavrijsen, D. M. F. Hartmann, A. van den Brink, Y. Yin, B. Barcones, R. A. Duine, M. A. Verheijen, H. J. M. Swagten, and B. Koopmans, *Phys. Rev. B* **91**, 104414 (2015).
- ³⁷C.-F. Pai, M. Mann, A. J. Tan, and G. S. D. Beach, *Phys. Rev. B* **93**, 144409 (2016).
- ³⁸K. Watanabe, S. Fukami, H. Sato, S. Ikeda, F. Matsukura, and H. Ohno, *Jpn. J. Appl. Phys., Part 1* **56**, 0802B2 (2017).
- ³⁹M. Bersweiler, H. Sato, and H. Ohno, *IEEE Magn. Lett.* **8**, 3109003 (2017).
- ⁴⁰S. Lemerle, J. Ferré, C. Chappert, V. Mathet, T. Giamarchi, and P. Le Doussal, *Phys. Rev. Lett.* **80**, 849 (1998).
- ⁴¹S. DuttaGupta, S. Fukami, C. Zhang, H. Sato, M. Yamanouchi, F. Matsukura, and H. Ohno, *Nat. Phys.* **12**, 333 (2016).
- ⁴²M. Vaňatka, J.-C. R. Sánchez, J. Vogel, M. Bonfim, M. Belmeguenai, Y. Roussigné, A. Stashkevich, A. Thiaville, and S. Pizzini, *J. Phys.: Condens. Matter* **27**, 326002 (2015).
- ⁴³D.-H. Kim, S.-C. Yoo, D.-Y. Kim, B.-C. Min, and S.-B. Choe, preprint [arXiv:1608.01762](https://arxiv.org/abs/1608.01762) (2016).
- ⁴⁴E. Jué, C. K. Safeer, M. Drouard, A. Lopez, P. Balint, L. B. Prejbeanu, O. Boulle, S. Auffret, A. Schuhl, A. Manchon, I. M. Miron, and G. Gaudin, *Nat. Mater.* **15**, 272 (2016).
- ⁴⁵D.-Y. Kim, M.-H. Park, Y.-K. Park, J.-S. Kim, Y.-S. Nam, D.-H. Kim, S.-G. Je, H.-C. Choi, B.-C. Min, and S.-B. Choe, *NPG Asia Mater.* **10**, e464 (2018).
- ⁴⁶D.-Y. Kim, D.-H. Kim, and S.-B. Choe, *Appl. Phys. Express* **9**, 053001 (2016).
- ⁴⁷H. T. Nembach, J. M. Shaw, M. Weiler, E. Jué, and T. J. Silva, *Nat. Phys.* **11**, 825 (2015).
- ⁴⁸X. Ma, G. Yu, C. Tang, X. Li, C. He, J. Shi, K. L. Wang, and X. Li, *Phys. Rev. Lett.* **120**, 157204 (2018).
- ⁴⁹A. Belabbes, G. Bihlmayer, F. Bechstedt, S. Blügel, and A. Manchon, *Phys. Rev. Lett.* **117**, 247202 (2016).
- ⁵⁰A. Belabbes, G. Bihlmayer, S. Blügel, and A. Manchon, *Sci. Rep.* **6**, 24634 (2016).
- ⁵¹R. Lo Conte, E. Martinez, A. Hrabec, A. Lamperti, T. Schulz, L. Nasi, L. Lazzarini, R. Mantovan, F. Maccherozzi, S. S. Dhesi, B. Ocker, C. H. Marrows, T. A. Moore, and M. Kläui, *Phys. Rev. B* **91**, 014433 (2015).
- ⁵²A. K. Chaurasiya, C. Banerjee, S. Pan, S. Sahoo, S. Choudhury, J. Sinha, and A. Barman, *Sci. Rep.* **6**, 32592 (2016).
- ⁵³G. Yu, P. Upadhyaya, K. L. Wong, W. Jiang, J. G. Alzate, J. Tang, P. K. Amiri, and K. L. Wang, *Phys. Rev. B* **89**, 104421 (2014).
- ⁵⁴S. Emori, E. Martinez, K.-J. Lee, H.-W. Lee, U. Bauer, S.-M. Ahn, P. Agrawal, D. C. Bono, and G. S. D. Beach, *Phys. Rev. B* **90**, 184427 (2014).